**To cite this article:** Wang W, Zhu S Y, He W P. Analysis on external pressure bearing capacity of cylindrical shell based on measured geometric defects[J/OL]. Chinese Journal of Ship Research, 2019, 14(4). http://www.ship-research.com/EN/Y2019/V14/I4/40.

**DOI:**10.19693/j.issn.1673-3185.01355

# Analysis on external pressure bearing capacity of cylindrical shell based on measured geometric defects

*Wang Wei*[1], *Zhu Shiyang*[*2], *He Weiping*[2]

1 Naval Military Representative Office in Huludao Area, Huludao 125004, China

2 Wuhan Second Ship Design and Research Institute, Wuhan 430205, China

**Abstract:** [**Objectives**] The purpose of this paper is to study the way to establish finite element models with real geometric defects, and to predict and analyze the bearing capacity of a scale down pressure- resisting cylindrical shell structure based on different types of defects. [**Methods**] Therefore, a geometric defect extraction method based on quadratic transformation is proposed, then the method of introducing the measured initial geometric defect, which is expressed by double Fourier series, is established. Finally, the buckling capacity of scale down pressure-resisting cylindrical shell under external pressure is analyzed and obtained based on eigenvalue modal defect and measured defect. [**Results**] The results indicate that Fourier series method only involves traversing of grid nodes and calculation of a few function values and can significantly improve the calculation efficiency of defect introduction without reducing the accuracy of calculation. [**Conclusions**] Fourier series method can provide guidance for accurate analysis of ultimate bearing capacity of cylindrical shell structure and structural optimization design.

**Key words:** cylindrical shell; bearing capacity; geometric defects; Fourier series

**CLC number:** U661.4

## 0 Introduction

In engineering structure, the cylindrical shell is widely applied, but it has obvious sensitivity to imperfections, leading to a great reduction and a large-range discrete distribution of buckling load. In actual engineering, the initial geometric deflects will inevitably occur in the production and transportation of cylindrical shell structure [1], which has a great influence on the bearing capacity of cylindrical shell structure, so it is necessary to analyze the bearing capacity of cylindrical shell based on the measured geometric deflects.

Related studies on this problem have been carried out abroad for a long time. By comparing the theoretical and experimental results, Southwell [2] observed that the measured buckling loads are always much smaller than the theoretical value of corresponding model. Von Karman and Tsien [3] proposed a more general solving method for post-buckling of cylindricalshells by solving the nonlinear large-deflection equation of cylindrical shells. Koiter [4] first proposed the perturbation theory to study and analyze the initial post-buckling path of linear elastic structure. Donnell and Wan [5] introduced the geometric deflects of cylindrical shell into the post-buckling analysis, and the calculated critical buckling load is much lower than that of the perfect/improved shell. To solve the buckling problem of thin cylindrical shell structure, some Chinese scholars have carried out a theoretical study on the solving method of large-deflection equation[6] and elastic-plastic buck-

**Received:** 2018-07-16

**Authors:** WANG Wei, male, born in 1982, master, engineer. Research interest: structural design of submarine. E-mail: 50788631@qq.com

ZHU Shiyang, male, born in 1990, master, engineer. Research interest: structural design of submarine. E-mail: zhushiyang@mail.dlut.edu.cn

HE Weiping, male, born in 1985, master, senior engineer. Research interest: structural design of submarine. E-mail: heweiping133@163.com

***Corresponding author:** ZHU Shiyang

ling of thin cylindrical shell [7-8]. The above studies show that in the case of initial imperfections, the ultimate bearing capacity of cylindrical shell is obviously different from the experimental results, and the experimental results have large random discreteness. Initial imperfections of the shell include initial geometric deflects, shell thickness imperfections, and load imperfections. However, there are many kinds of real imperfections, which have gone beyond the scope of classical geometric deflects. However, the non-classical geometric deflects lead to more complex and variable factors affecting the critical buckling load of the structure, thus greatly increasing the difficulty of shell structure design. Other common imperfections include the linear buckling mode imperfection (LBMI), axial symmetry imperfection (ASI), and measured imperfection (MI). Among them, LBMI is widely applied in the field of civil engineering for the buckling analysis of thin shell structures such as oil tanks with wind load, cooling towers with axial compression, and carrier rockets. In addition, LBMI is also utilized in the reduction stiffness analysis. One of the reasons why LBMI is widely applied is that it is easy to obtain the imperfections using the general finite element (FE) software for the linear buckling analysis of structure. ASI is now more commonly used for the comparative analysis of imperfection sensitivity. MI is mainly to obtain the point cloud data of surface morphology for shell structures by contact or non-contact measurement methods and to introduce the imperfection into the FE analysis. In the field of MI study, Arbocz and Abramovich [9] have made great contributions to the establishment of the initial imperfection database.

The study of the nonlinear buckling theory and the ultimate bearing capacity analysis of underwater ring-stiffened cylindrical shell structure under severe running conditions started relatively late in China. Not only the analysis method is single, but also the accuracy is insufficient, and the test data are relatively scarce, especially in the analysis of structural bearing capacity involving the measured initial geometric deflects. Therefore, in this paper, the initial geometric deflects of the shell are firstly extracted based on the quadratic transformation method to measure the initial geometric deflects of cylindricalshells. Then the FE model is reconstructed using the double Fourier series method to analyze the effect of initial geometric deflects on the external pressure bearing capacity of cylindrical shell. Finally, the differences in the calculation accuracy and efficiency between the two reconstruction methods for FE models are compared and analyzed.

## 1 Measurement and expression of geometric deflects

In this paper, the 3D topography results of the surface of samples are obtained using 3D topography measurement system, and the point cloud form is shown in Fig. 1. However, in the actual application of these point cloud data, the measurement coordinate system of point cloud data is not consistent with the coordinate system of simulation modeling of the sample. Therefore, the coordinate transformation is also required to obtain the expected spatial position, as shown in Fig. 2.

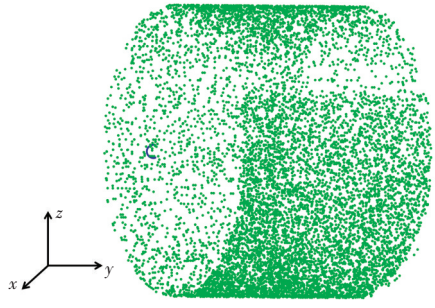


Fig.1 3D topography data acquired from 3D measurement system

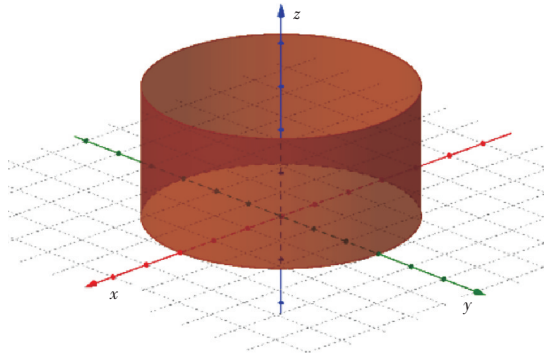


Fig.2 Expected spatial position of 3D topography data

Although the overall topography point cloud information of the cylindrical shell surface can be obtained based on 3D topography measurement system, characteristic parameters including the radius of cylindrical shell and axial direction cannot be directly obtained. Therefore, in this paper, the overall topography point cloud information of the cylindrical shell surface output by 3D topography measurement system is firstly fitted using the least square method, and the general equation of the quadratic surface is obtained. Then the measurement coordinate system of the point cloud is transformed into the standard reference coordinate system adopted for FE modeling by the orthogonal transformation. In addition, the

fitted value of cylindrical shell diameter can be obtained directly by analyzing the quadratic coefficients.

Fig. 3 shows the coordinate systems adopted in this paper. $O-XYZ$ is the measurement coordinate system; $O'-X'Y'Z'$ is the standard coordinate system (modeling coordinate system); $O'-r\theta y$ ( $r, \theta, y$ refers to the radial direction, circumferential direction, and axial coordinate respectively) is the coordinate system of the standard cylindrical shell. In the figure, $A$ is the customized calibration point. In this paper, the intersection point of the first quadrant and the lower end face of the external surface of the cylindrical shell is taken.

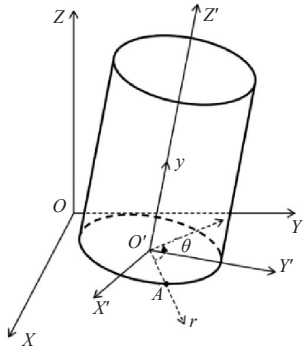


Fig. 3 Definition of the coordinate systems in this paper

In the measurement coordinate system, the cylindrical shell can be described by the general ternary quadratic surface equation, i.e.,

$$\boldsymbol{F}(x,y,z)=a_{11}x^2+a_{22}y^2+a_{33}z^2+2a_{12}xy+2a_{13}xz+2a_{23}yz+2a_{14}x+2a_{24}y+2a_{34}z+a_{44}=0 \quad (1)$$

The matrix form is written as

$$\boldsymbol{F}(x,y,z)=\boldsymbol{X}^{\mathrm{T}}\boldsymbol{A}\boldsymbol{X}+2\boldsymbol{b}\boldsymbol{X}+a_{44}=0 \quad (2)$$

where

$$\boldsymbol{A}=\begin{bmatrix}a_{11} & a_{12} & a_{13}\\ a_{21} & a_{22} & a_{23}\\ a_{31} & a_{32} & a_{33}\end{bmatrix},\ \boldsymbol{X}=(x\ y\ z)^{\mathrm{T}},\ \boldsymbol{b}=(a_{14}\ a_{24}\ a_{34})$$

where $\boldsymbol{A}$ is the symmetric matrix of the characteristic coefficient of the quadratic equation; $\boldsymbol{X}$ is the independent variable matrix, $\boldsymbol{b}$ is the one-degree term coefficient vector; $a_{11}-a_{33}$ are the coefficients; $a_{44}$ is the constant term.

Through the cross calculation of coordinate values, the solution of the ternary quadratic surface equation shown in Eq. (1) can be transformed into the problem of multiple linear fitting. In the fitting process, the coefficient matrix of the quadratic equation is obtained by the least square method. Since $\boldsymbol{A}$ is a real symmetric matrix, there is an orthogonal matrix $\boldsymbol{R}_0$.

$$\boldsymbol{R}_0^{\mathrm{T}}\boldsymbol{A}\boldsymbol{R}_0=\boldsymbol{\Lambda} \quad (3)$$

where $\boldsymbol{\Lambda}$ is the diagonal matrix.

Further, Eq. (2) can be transformed into Eq. (4) in the standard coordinate system.

$$\boldsymbol{F}(x,y,z)=\boldsymbol{X}'^{\mathrm{T}}\boldsymbol{\Lambda}\boldsymbol{X}'+2\boldsymbol{c}\boldsymbol{X}'+a_{44}=0$$

where

$$\boldsymbol{X}=\boldsymbol{R}_0\boldsymbol{X}',\quad \boldsymbol{c}=\boldsymbol{b}\boldsymbol{R}_0 \quad (4)$$

where $\boldsymbol{c}$ is the one-degree term coefficient vector.

The general equation of the quadratic surface is transformed into the standard equation through the orthogonal transformation [10]. The transformation eliminates the cross term between coordinate components and aligns the direction of the measurement coordinate system with the standard coordinate system by correcting the additional feature points, so as to keep the surface shape unchanged at the same time.

The point cloud in the standard coordinate system is transformed into the coordinate system of standard cylindrical shell, and the distance (off-plane displacement $w$ ) between scattered points in the topography point cloud and the fitting surface is calculated, as shown in Fig. 4. The off-plane displacement field $w(x,y)$ contains the initial geometric deflect information of the shell, which is also the data foundation for subsequent studies. In the figure, $\theta$ is the circumferential angle; $\bar{W}$ is the normalized dimensionless off-plane displacement $\bar{W}(x,y)=w(x,y)/t$ ; $t$ is the thickness of cylindrical shell); $L$ is the nominal length of the cylindrical shell.

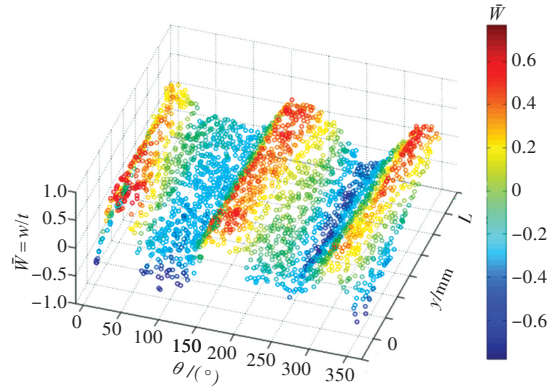


Fig.4 Scattered points diagram of initial geometric defects in cylinder coordinate system

The real imperfections of cylindrical shell structure have a great effect on the structural bearing capacity, which is a hot spot and difficulty for studies over the years. Scholars all over the world usually expand the real imperfections of cylindrical shell [off-plane displacement field $w(x,y)$ ] into a double Fourier series of half-wave cosine or half-wave sine.

In the coordinate system of finite element, the double Fourier series of half-wave cosine and half-wave

sine are respectively expressed as

$$w(x,y)=t\cdot\bar{W}(x,y)=$$
$$t^{*}\sum_{k=0}^{n_1}\sum_{l=0}^{n_2}\cos\frac{k\pi x}{L}\left(A_{kl}\cos\frac{ly}{R}+B_{kl}\sin\frac{ly}{R}\right) \quad (5)$$

$$w(x,y)=t\cdot\bar{W}(x,y)=$$
$$t^{*}\sum_{k=0}^{n_1}\sum_{l=0}^{n_2}\sin\frac{k\pi x}{L}\left(C_{kl}\cos\frac{ly}{R}+D_{kl}\sin\frac{ly}{R}\right) \quad (6)$$

where $R$ is the nominal radius of cylindrical shell; $A_{kl}$ and $B_{kl}$ are Fourier series coefficients of half-wave cosine; $C_{kl}$ and $D_{kl}$ are Fourier series coefficients of half-wave sine; $k$ and $l$ refer to axial half-wavenumber and circumferential full wavenumber respectively; $n_1$ and $n_2$ are the number of double Fourier series.

## 2 Bearing capacity analysis of cylindrical shell under axial compression

In order to obtain the actual buckling load of cylindrical shell, it is necessary to introduce the measured geometric deflects into the FE model, so as to reconstruct the perfect model into the FE model with measured geometric deflects. The reconstruction methods of the FE model include the FE model correction method based on the scattered points and FE model reconstruction method based on the Fourier series function. The latter is called the Fourier series method in this paper, which introduces MI in the form of the Fourier series. Specifically, the measured geometric deflects are expressed in the form of Fourier series, and then the Fourier series is introduced into the FE model to modify node coordinates, so as to introduce the measured geometric deflects.

Firstly, in this paper, the point cloud information in the cylindrical shell coordinate system shown in Fig. 4 is interpolated by the weighted interpolation of inverse distance, and the off-plane displacement diagram in grille form is obtained as shown in Fig. 5. Thus, the off-plane displacement field is expressed as the form of 2D matrix.

Then, the two-dimensional matrix is periodically extended and filtered by Gaussian filter in order to reduce the interference of measurement noise, and the off-plane displacement results after Gaussian noise reduction are shown in Fig. 6. In the figure, the black dots are the original scattered data. Fig. 6 shows that the off-plane displacement field in grille form and after noise reduction can well reflect the measured topography represented by the original scattered points.

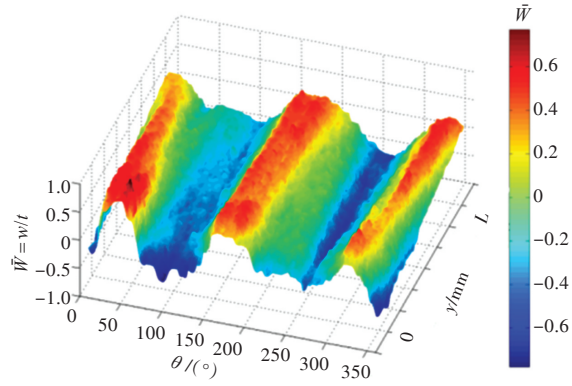


Fig.5 Off-plane displacement diagram in grille form of cylindrical shell

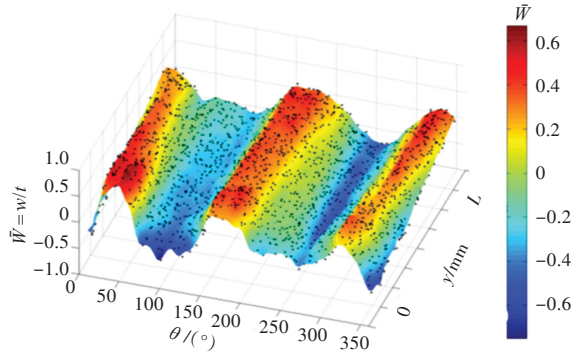


Fig.6 Off-plane displacement diagram of cylindrical shell after Gaussian noise reduction

Finally, the obtained Fourier series coefficients $A_{kl}$ and $B_{kl}$ of half-wave cosine are saved in file form, and Python script is written to read the coefficients. MI is introduced in the ABAQUS FE model using the Fourier series represented by the coefficients, so as to realize the reconstruction of the FE model with MI. Fig. 7 shows the reconstructed FE model, and the amplitude of MI is magnified by 30 times in consideration of the display effect.

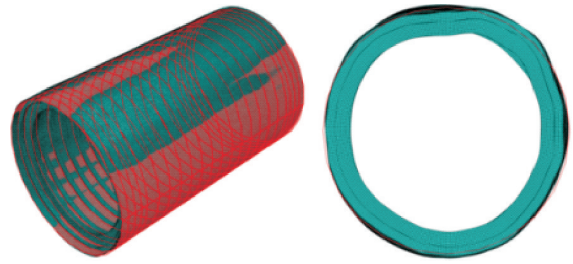

Fig.7 FE model of reconfigured cylindrical shell with measured defects

### 2.1 Numerical analysis of bearing capacity of the perfect model

The perfect model presented in this paper refers to the improved cylindrical shell model without MI. The nominal radius $R$ of the perfect cylindrical shell model is the fitting radius obtained by the feature extraction of the measured topography of the actual

structure. Fig. 8 shows the boundary conditions and loads of the model.

Fig.8 Boundary conditions of cylindrical shell FE model

In Fig. 8, the bottom of model is a fixed support to restrict three linear displacements and three rotational degrees of freedom of the nodes on the bottom frame of the model. The upper end only loosens the axial displacement degree of freedom and restricts the other five degrees of freedom. The uniformly distributed pressure load is applied to the external surface of model, and the axial load is applied to the end face in consideration of the nonlinear deformation of structure. The mesh size is set reasonably through the mesh convergence analysis, and the bilinear elastic-plastic model is used for material properties.

The calculation results show that the FE model of the perfect cylindrical shell has the ultimate bearing capacity $P_{\text{perfect}}$ = 0.835 7 (the normalized dimensionless pressure load based on the theoretical ultimate bearing capacity, the same below), and the displacement - loading curve is shown in Fig. 9. As can be seen from Fig. 9, the OA segment is the linear pre-buckling stage of cylindrical shell, and the bearing capacity increases linearly with the increase in displacement-load. Local shell buckling occurs when the maximum value is reached at point A (critical instability state). As the displacement-load continues to increase, the bearing capacity gradually decreases and becomes stable at point B (a large deformation state after collapse).

## 2.2 Approximate analysis of mode imperfection

Since the initial geometrical imperfections in mode or shape-like modes have a great effect on the critical buckling load of the structure under axial compression, the mode imperfection approach is also one of the important methods used in the prediction and analysis of the bearing capacity of the cylindrical shell structure. This method mainly aims at the structure whose initial imperfection form is not very clear, and we usually use the first-order mode of the structure to simulate the initial geometric deflects of the structure. Because the results of this method are not always in good agreement with the experimental data, it is generally used to calculate the lower limit bearing capacity of the structure.

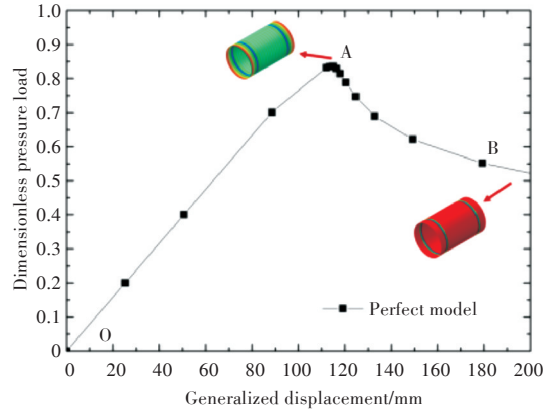


Fig.9 Displacement-loading curve of perfect cylindrical shell FE model

Here, the FE model of cylindrical shell in Section 2.1 is used to apply the normalized displacement-load to the model, and the linear buckling analysis step is established. To introduce the buckling mode imperfections, the INP file of linear buckling analysis is modified to increase the output of the nodal displacement vector. After the linear buckling analysis, a new Riks analysis step is built and a command is added to the corresponding INP file to introduce the results of linear buckling analysis, and then the calculation of ultimate bearing capacity is started. Related processes and commands are as follows.

1) Before the linear buckling analysis, the following commands are added to the INP file. After the calculation, a file with the extension fil will be generated in the working directory, which will be used in the next step.

```
*Node File
U,
```

2) The mode imperfection file of the previous step is introduced using the following commands:

```
Imperfection,file=FileName,
Step=StepNumber
1,ScalingFactor
```

where the FileName is the filename (without the extension) of the previous fil file. StepNumber must be the same as that in the model of the previous step, and ScalingFactor is usually 1.

3) Load under axial external pressure is applied, calculated and analyzed.

First-order local mode imperfection and first-order global mode imperfection as shown in Fig. 10 are introduced with the imperfection amplitude of $0.2t$ and $0.002\,5R$ respectively, and the displacement-loading curves of cylindrical shell are obtained as shown in Fig. 11.

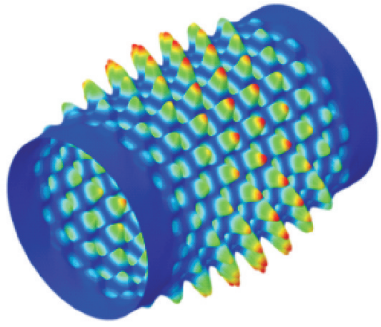

(a) First-order local mode imperfection

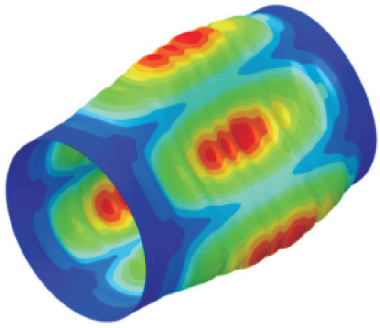

(b) First-order global mode imperfection

Fig.10 The first-order mode defects of cylindrical shell

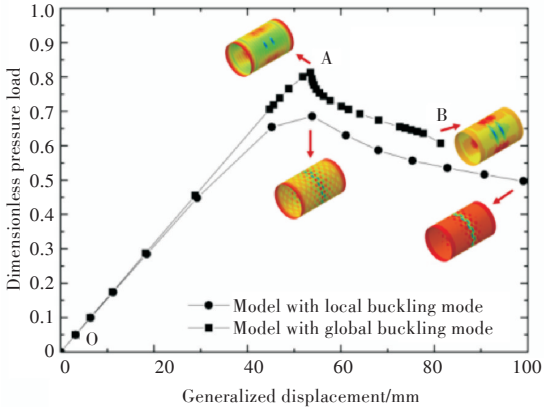


Fig.11 Displacement-loading curves of cylindrical shell FE model considering mode defects

As can be seen from Fig. 11, the OA segment is in the linear pre-buckling stage, and the bearing capacity of cylindrical shell has a basically linear relationship with displacement-load. With the increase in the displacement-load, the cylindrical shell enters into the nonlinear post-buckling stage (AB segment), in which the bearing capacity of cylindrical shell also has a basically linear relationship with the displacement-load, but the static stiffness of structure obviously decreases. As the generalized displacement increases, the maximum bearing capacity $P_{\text{local}}$ and $P_{\text{global}}$ of cylindrical shell decrease to 0.812 5 and 0.685 3 respectively, and then the shell buckling occurs, and the shell deformations caused by these two mode imperfections have certain differences.

## 2.3 Approximate analysis of MI

Because MI truly reflects the initial geometric deflects of cylindrical shell structure, the ultimate bearing capacity analysis based on the MI of structure can predict the ultimate bearing capacity very accurately. The method used in this paper is the measured imperfection approach (MIA).

Here, the same FE model as that in Section 2.1 is adopted. The topography of cylindrical shell is measured, analyzed and expressed using the topography measurement method for large cylindrical shell structures. The MI is introduced through the FE model correction method based on scattered points or Fourier series function, and the FE model of cylindrical shell with MI as shown in Fig. 7 above is obtained.

According to the results of the ultimate bearing capacity analysis of FE model of cylindrical shell using the scattered point method and Fourier series method, the ultimate bearing capacity $P_{\text{Point}}$ and $P_{\text{Fourier}}$ of cylindrical shell obtained by the two methods are 0.824 2 and 0.823 8 respectively in consideration of MI, as shown in Fig. 12. As can be seen from Fig. 12, the results calculated by the scattered point method and Fourier series method are almost identical. In the OA segment, the cylindrical shell is in the linear pre-buckling stage, and the bearing capacity increases linearly with the increase in the displacement-load. Local buckling occurs when the maximum bearing capacity reaches 0.824 2. In the nonlinear post-buckling stage (AB segment), the structure gradually changes from the local buckling to the circumferential buckling of intercostal shell, and the bearing capacity decreases to about 0.4.

## 2.4 Comparison of two reconstruction methods

The same MI is introduced using the two FE model reconstruction methods, namely the scattered point method and Fourier series method. The ultimate bearing capacity is analyzed after the FE model of cylindrical shell is reconstructed, and the performance comparison of the two reconstruction methods

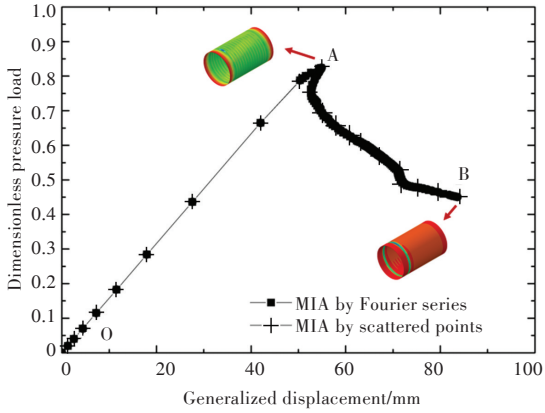


Fig.12 Displacement-loading curve of cylindrical shell FE model considering measured defects

is shown in Fig. 13. In the figure, the solid lines represent the buckling loads (normalized dimensionless results) of cylindrical shells with different mesh sizes determined by the two methods, and the dotted lines represent the time cost by the two methods to introduce the imperfections. Fig. 13 shows that there is almost no difference in buckling loads of cylindrical shell with different mesh sizes determined by the two methods, and the process of introducing imperfections by the scattered point method takes much longer than using Fourier series method. With the increase in the mesh number, the time of introducing imperfections increases exponentially, and the difference between the two is more obvious. The maximum time consumption of Fourier series method is 48% of that of the scattered point method, and the average time consumption is 32% of that of the scattered point method. It can be seen that the overall computational efficiency of the Fourier series method is higher than that of the scatter point method. It can be seen that the overall computational efficiency of Fourier series method is higher than that of the scattered point method.

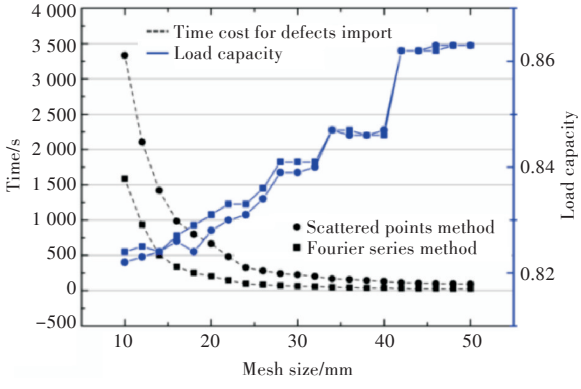


Fig.13 Mesh convergence rate curves and time cost by two methods

## 3 Conclusions

In this paper, the numerical analysis is carried out on the bearing capacity of cylindrical shell under external pressures with initial geometric deflects, and the main conclusions are as follows:

1) The orthogonal transformation based on quadratic form and the initial geometric deflect expression method of Fourier series can solve the problem of disunity from measurement coordinate system to modeling coordinate system, thus forming the FE model reconstruction method based on the measured geometric deflects.

2) The computational efficiency of Fourier series method is significantly higher than that of the scattered point method, which can save at least 52% of time in the imperfection introduction process, and the efficiency advantage will be more obvious with the increase in the computing scale.

3) The ultimate bearing capacity of cylindrical shell based on mode imperfection is more conservative than that based on MI, and it can be used as the lower limit value of ultimate bearing capacity. However, MI is the combination of various mode imperfections, and the ultimate bearing capacity of cylindrical shell based on MI is closer to the actual value, which can provide guidance for the accurate analysis of ultimate bearing capacity and optimization design of cylindrical shell structure.

4) The ultimate bearing capacity of cylindrical shell is more sensitive to the local mode imperfections than the global mode imperfections. In the process of construction, the shape misalignment of intercostalshells caused by welding deformation and manufacturing should be strictly controlled to ensure the bearing capacity of cylindricalshells.

## References

[1] Huang J Q. Shape analysis of ring-stiffened cone-toroid-cylinder combined shells' initial geometrical imperfection [J]. Chinese Journal of Ship Research, 2015, 10(3): 51-56 (in Chinese).

[2] Southwell R V. On the general theory of elastic stability [J]. Philosophical Transactions of the Royal Society A: Mathematical, Physical and Engineering Sciences, 1914, 213(497-508): 187-244.

[3] Von Karman T, Tsien H S. The buckling of thin cylindrical shells under axial compression [J]. Journal of Aeronautic Science, 1941, 8(8): 302.

[4] Koiter W T. On the stability of elastic equilibrium [D]. Delft: Delft University of Technology, 1945.

[5] Donnell L H, Wan C C. Effect of imperfections on

buckling of thin cylinders and columns under axial compression [J]. Journal of Applied Mechanics, 1950, 17(1): 73-83.
[6] Hu H C. Variational principles in elasticity and their applications[M]. Beijing: Science Press, 1981 (in Chinese).
[7] Zhou C C. Theory of elastic-plastic stability for thin shells [M]. Beijing: National Defense Industry Press, 1979 (in Chinese).
[8] Huang K Z, Xia Z X, Xue M D, et al. Theory of plates and shells [M]. Beijing: Tsinghua University Press, 1987 (in Chinese).
[9] Arbocz J, Abramovich H. The initial imperfection data bank at the Delft University of Technology: Part I[R]. Delft Netherlands: Delft University of Technology, 1979: 1-18.
[10] Zhang X, Hu C H, Chen W Y. Quadratic surface fitting and uncertainty analysis of fitting parameters[J]. Journal of Beijing University of Aeronautics and Astronautics, 2006, 32(9): 1091-1095 (in Chinese).

# 基于实测几何缺陷的圆柱壳外压承载能力分析

王伟[1], 朱时洋[*2], 和卫平[2]
1 海军驻葫芦岛地区军事代表室,辽宁 葫芦岛 125004
2 武汉第二船舶设计研究所,湖北 武汉 430205

**摘 要**:[**目的**]为研究含真实几何缺陷的有限元模型建立途径,并基于不同类型缺陷对某缩比耐压圆柱壳结构的承载性能进行预测分析,[**方法**]提出基于二次型变换的几何缺陷提取方法,利用双重傅里叶级数表达实测初始几何缺陷,建立实测初始几何缺陷的引入方法。根据特征值模态型缺陷和实测缺陷,分别分析获得的缩比耐压圆柱壳的外压屈曲承载能力。[**结果**]结果显示,傅里叶级数法在不降低计算精度的前提下仅涉及网格节点的遍历和少量函数值的计算,使缺陷引入的计算效率得到显著提高。[**结论**]傅里叶级数法能够为圆柱壳结构极限承载能力的精确分析及结构优化设计提供指导。

**关键词**: 圆柱壳; 承载能力; 几何缺陷; 傅里叶级数

[*Continued from page* 15]

nal of Ship Research, 2014, 9(4): 55-62 (in Chinese).
[14] Cao B Z, Ling Y K, Jiang H Z, et al. Warhead and fuze of aerodynamic missile[M]. Beijing: Aerospace Publishing House, 1995 (in Chinese).

# 高硬度聚脲涂覆FRC复合结构抗冲击性能试验分析

赵鹏铎[*1], 贾子健[1,2], 王志军[2], 张磊[1], 徐豫新[3], 张鹏[1,2]
1 海军研究院, 北京 100161
2 中北大学 机电工程学院 ,山西 太原 030051
3 北京理工大学 爆炸科学与技术国家重点试验室, 北京 100081

**摘 要**:[**目的**]为了分析玻璃纤维—芳纶(FRC)底材涂覆硬质聚脲的复合结构的抗冲击性能,[**方法**]采用口径12.7 mm的弹道枪进行破片冲击加载,得到破片的弹道极限速度,分析获得不同工况下复合结构靶板的极限比吸收能。在此基础上,结合靶板的宏观破坏形貌,讨论2种不同聚脲涂覆复合结构的抗冲击性能的优劣性,并与软质聚脲涂覆复合结构进行对比,以验证涂覆硬质聚脲复合结构的最佳抗冲击性能。[**结果**]研究表明,作为背弹面涂层时,软质聚脲涂覆复合结构的抗冲击性能较好;作为迎弹面涂层时,硬质聚脲涂覆复合结构的抗冲击性能较好;两种聚脲涂层作为迎弹面的复合结构抗冲击性均优于背弹面和双面复合结构。[**结论**]在一般工程应用防护中,选用高硬度聚脲材料作为迎弹面涂层的防护效果更好。

**关键词**:抗爆抗冲击; 复合材料; 高硬度聚脲; 软质聚脲; 防护结构; 弹道极限速度